Supporting Information

Barry et al. 10.1073/pnas.1000406107

SI Text

Materials and Methods. Virus was grown using standard biological techniques (1). These procedures yielded virus stock solutions that had a low volume fraction of multimers, such as dimers that have a contour length that is twice that of *fd wt*. The presence of these longer viruses was found to dramatically influence the phase diagram by stabilizing smectic filaments and surface-induced smectic phase while suppressing the formation of colloidal membranes (2). These longer rods act as a natural bridge that bridges multiple membranes thus altering their stability with respect to smectic filaments. Experimentally, we find that rod-like particles with a high degree of monodispersity are essential for reproducible assembly of colloidal membranes. To further fractionate the viruses used in this study, samples were prepared at isotropic-nematic phase coexistence so that 20% of the sample is nematic and the rest is isotropic. Longer rods preferentially dissolve in the nematic phase (3). Only isolated isotropic fractions were used for our studies, thus significantly extending the region of the phase diagram in which assembly of isolated membranes is observed.

Particles were fluorescently labeled using Alexa 488 (Molecular Probes) as described elsewhere (4). Dextran was used as a depletant (molecular weight 500,000, SimgaAldrich), and all samples were made in a 100-mM NaCl and 20-mM Tris buffer at pH = 8.0. Samples were prepared between glass cover slides and coverslips in homemade chambers. A layer of unstretched Parafilm was used as a spacer. To suppress nonspecific binding of the membranes to one of the surfaces, glass slides were cleaned in hot soap solution (Hellmanex) and subsequently dipped into a hot dissolved agarose suspension (0.01 mg/mL). Samples were made airtight using UV treated glue (Norland Optical) and stored at 4 °C. All data reported here were taken within days of sample preparation, although samples were typically good for months to years. Sample behavior was examined using an inverted microscope (Nikon TE 2000) with either water (60×, NA 1.2) or oil immersion objectives (100×, PlanFluor NA 1.3). Data were acquired using a cooled CCD camera (either CoolSnap HQ or Andox iXon 897). Dual-View (Photometrics) was used to simultaneously acquire fluorescence and phase contrast/differential interference contrast (DIC) images. The data were analyzed with software written in the Interactive Data Language programming language (RSI).

For analysis of the membrane's fluctuations at continuum lengthscales, we have used exposure times of 1 ms in order to reduce the artifacts associated with image blurring that becomes significant during longer exposure times. This unfortunately is not possible when using Dual-View in order to image protrusion interactions. Fluorescence images with adequate signal to noise require integration times of up to a few hundred milliseconds. Under Dual-View, the exposure time for bright field imaging and fluorescence imaging is the same. These long exposure times result in substantial blurring of the images, which significantly reduces the accuracy of the data taken with this imaging modality. For these reasons, although qualitative features of data shown in Fig. 4*D* are correct, greater caution is required when quantitatively interpreting protrusion fluctuations.

We have used two different protocols to obtain membranes in the edge-on and face-on configurations. To observe membranes in a face-on configuration, we have extensively cleaned the coverslip and cover-glass surfaces according to previously published protocols (5). Subsequently, we have made these surfaces nonadsorbing by dipping them into a hot solution of molten agarose, which coats the surface with a thick polymer brush and thus prevents adsorption of the membrane on the surface. Because of their high density, membranes slowly sediment onto the coverslip surface. Most of these membranes spread on the surface in a face-on configuration. We have used a sequence of these image to measure the fluctuations of the membrane area. There are two possible sources of these fluctuations. The first possibility is that a membrane locally desorbs from the coverslip surface, which consequently decreases the measured (projected) area. The second possibility is that the background polymer exerts a constant osmotic pressure on membranes. Similar to other assemblages at constant pressure, the membrane area will fluctuate due to its finite compressibility. We can distinguish between these two possibilities by measuring the local desorption of membranes with total internal reflection florescence (TIRF) microscopy in which all the viruses are fluorescently labeled. In TIRF images, the brightness of a membrane is directly proportional to its distance from a surface. We observe that the intensity of membranes viewed in such a way does not change on relevant time scales. Therefore, we conclude that the weight of the membrane suppresses bending fluctuations, and changes in the area are almost entirely due to density fluctuations associated with the finite compressibility of the membranes.

To image membranes in edge-on configurations we have used two different methods. In one method, we have prepared the samples in agarose-coated chambers and allow the membranes to sediment onto the coverslip surface. A few hours before the measurement, we invert the sample, which causes the membranes to peal away from the agarose-treated surface and slowly sediment away from the coverslip. During the sedimentation process we frequently observe free membranes in edge-on configurations. To measure the bending rigidity we analyze the fluctuations of these membranes while ensuring that our data are taken sufficiently far away from free edges. During the time it takes to acquire data, the sedimentation of the membranes is negligible. We have also developed an alternative method to observe a high fraction of membranes in the edge-on configuration. In these samples, we have avoided treating the samples with molten agarose. This results in an attractive depletion interaction between coverslip surface and virus particles. As a result, a monolayer of rods covers the coverslip surface. These rods act as a nucleation site for the formation of membranes that grow away from the surface into the bulk of the samples. Consequently, in these samples we observe a high-volume fraction of membranes in edge-on configuration. We again ensure that our data are taken sufficiently far away from edges that are either free or attached to the coverslip surface. Using both methods, we measure the bending rigidity of the membranes that are in reasonable agreement with each other.

1. Maniatis T, Sambrook J, Fritsch E, eds (1989) *Molecular Cloning* (Cold Spring Harbor Lab Press, Cold Spring Harbor, NY).
2. Dogic Z (2003) Surface freezing and a two-step pathway of the isotropic-smectic phase transition in colloidal rods. *Phys Rev Lett* 91:165701.
3. Lekkerkerker HNW, et al. (1984) On the isotropic-liqud crystal phase-separation in a solution of rodlike particles of different lengths. *J Chem Phys* 80:3427–3433.
4. Lettinga MP, Barry E, Dogic Z (2005) Self-diffusion of rod-like viruses in the nematic phase. *Europhys Lett* 71:692–698.
5. Lau AWC, Prasad A, and Dogic Z (2009) Condensation of isolated semi-flexible filaments driven by depletion interactions. *Europhys Lett* 87:48006.

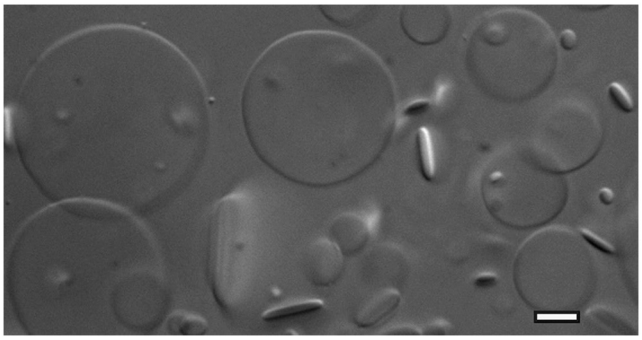

Movie S1. DIC video of a virus/polymer suspension that contains numerous membranes. These membranes eventually coalesce to form large monolayers that can be up to hundreds of microns in diameter. During the movie we switch between DIC imaging, which reveals continuum fluctuations of the membranes, and fluorescence imaging, which uncovers molecular dynamics of fluorescently labeled rods that are present at low-volume fraction.
Movie S1 (AVI)

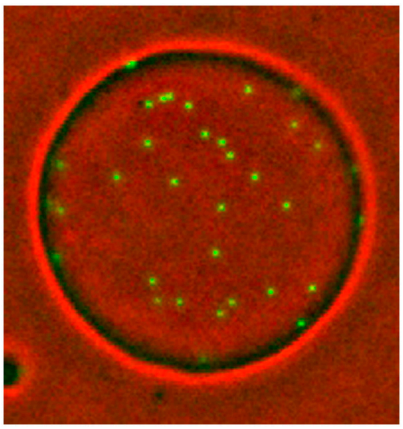

Movie S2. Composite phase contrast/florescence video of a membrane viewed in a face-on configuration. Approximately 1 particle out of 30,000 particles is fluorescently labeled. Phase contrast and florescence images are acquired simultaneously and are subsequently overlaid with nanometer precision. Fluorescently labeled rods within the membrane are viewed along their axial directions and appear as green isotropic spots. The diameter of the membrane shown is 15 μm. The video is sped up by a factor of 2.
Movie S2 (AVI)

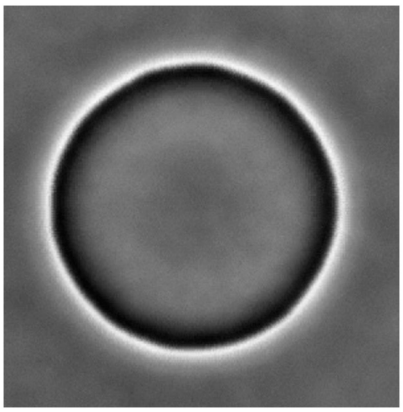

Movie S3. Video of a membrane viewed in a face-on configuration and acquired using phase contrast microscopy. Fluctuations in the membrane area are used to extract a compressibility modulus for the membrane. The diameter of the membrane shown is 11 μm. The video is sped up by a factor of 3.
Movie S3 (AVI)

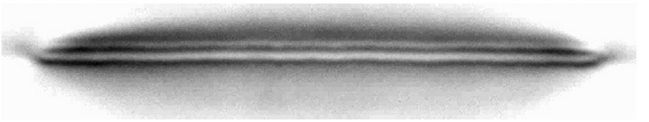

Movie S4. Video of a membrane viewed in an edge-on configuration (surface normal lying in the plane of the screen). This video is acquired using DIC microscopy, and the image is focused on the midplane of the membrane. Visible thermal undulations of the membrane are used to extract its bending modulus (Fig. 3). The diameter of the membrane shown is 16 μm. The video is shown in real time.

Movie S4 (AVI)

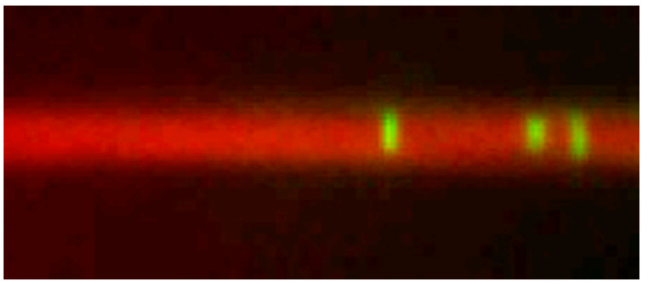

Movie S5. Composite polarization/florescence video of a membrane viewed in an edge-on configuration. Polarization and florescence images are acquired simultaneously and are subsequently overlaid with nanometer precision. Protrusion fluctuations of individual rods within the membrane are measured from similar movies (Fig. 3). The video is shown in real time.

Movie S5 (AVI)